


Design of monopole antennas based on progressive Gaussian process

cambridge.org/mrf

Xie Zheng^{1,*} , Fei Meng^{2,*}, Yubo Tian² and Xinyu Zhang¹

¹School of Electronics and Information, Jiangsu University of Science and Technology, Zhenjiang 212100, Jiangsu, China and ²School of Information and Communication Engineering, Guangzhou Maritime University, Guangzhou 510725, Guangdong, China

Research Paper

*Xie Zheng and Fei Meng are co-first authors.

Cite this article: Zheng X, Meng F, Tian Y, Zhang X (2023). Design of monopole antennas based on progressive Gaussian process. *International Journal of Microwave and Wireless Technologies* **15**, 255–262. <https://doi.org/10.1017/S1759078722000125>

Received: 11 June 2020
Revised: 12 January 2022
Accepted: 14 January 2022
First published online: 7 March 2022

Key words:

Electromagnetic simulation; Gaussian process; surrogate model

Author for correspondence:

Yubo Tian, E-mail: tianyubo@just.edu.cn

Abstract

Electromagnetic simulation software has become an important tool for antenna design. However, high-fidelity simulation of wideband or ultra-wideband antennas is very expensive. Therefore, antenna optimization design by using an electromagnetic solver may be limited due to its high computational cost. This problem can be alleviated by the utilization of fast and accurate surrogate models. Unfortunately, conventional surrogate models for antenna design are usually prohibitive because training data acquisition is time-consuming. In order to solve the problem, a modeling method named progressive Gaussian process (PGP) is proposed in this study. Specially, when a Gaussian process (GP) is trained, test sample with the largest predictive variance is inputted into an electromagnetic solver to simulate its results. After that, the test sample is added to the training set to train the GP progressively. The process can incrementally increase some important trusted training data and improve the model generalization performance. Based on the proposed PGP, two monopole antennas are optimized. The optimization results show effectiveness and efficiency of the method.

Introduction

Full-wave electromagnetic simulation software is one of the important tools in the field of antenna engineering, and the goal is to adjust geometry and/or material parameters to ensure the antenna satisfies design indexes. Usually, the problem of antenna design can be considered as an optimization problem. Among various optimization methods, the evolutionary algorithm, including particle swarm optimization (PSO), genetic algorithm, etc., is widely used due to its high global optimization ability, without good initial design, wide applicability, and robustness [1–3]. However, the optimization algorithm might require thousands of fitness function evaluations, namely, full-wave electromagnetic analysis of the optimized antenna, which is very time-consuming.

In order to solve the problem, surrogate-based optimization is applied to microstrip antennas (MSAs) or filter design [4, 5], which use surrogate models instead of high-fidelity electromagnetic simulation, significantly reducing the computational costs. Currently, the most common and popular surrogate models include artificial neural networks (ANNs) [6, 7], support vector machine (SVM) [8, 9], and Gaussian process (GP) [10, 11]. Chen *et al.* [12] used PSO parallelization to accelerate ANN training and simulate the resonant frequency of rectangular MSAs under the unified device architecture. Chen *et al.* [13] proposed an ANN based on prior knowledge to design the filter on an advanced design system. Angiulli *et al.* [14] proposed a SVM-based microwave device modeling. Sun *et al.* [15] gave a SVM combined with a hybrid kernel function for accurately modeling the resonant frequency of a compact MSA. Jacobs *et al.* [16] used a GP to model ultra-wideband (UWB) and dual-frequency coplanar waveguide (CPW) feed slot antennas. Gao *et al.* [17] proposed a semi-supervised co-training algorithm based on GP and SVM. Zhang *et al.* [18] constructed a deep GP model by using the structural form of convolutional neural networks and combining it with GP. Chen *et al.* [19] developed a manifold GP machine learning method based on a differential evolution algorithm. Gao *et al.* [20] gave a semi-supervised learning GP, which combines unlabeled samples to improve the accuracy of the GP model and reduce the number of labeled training samples required. Zhou *et al.* [21] presented a novel surrogate-assisted evolutionary optimization framework that combines both global and local surrogate models.

Although these proposed methods can reduce the number of evaluations of electromagnetic simulations, it is also a deserved research topic. In this paper, we primarily propose a progressive GP (PGP) to solve the problem of insufficient generalization ability of GP model when modeling some antennas with complex structure. The main research details of this paper are as follows:

- (1) By the method of orthogonal experiment design, we generate a small number of samples which is training set to train a GP model. Progressively, some new samples with large variances predicted by the trained GP are simulated by using electromagnetic software, such as high-frequency structure simulator (HFSS) (<https://www.ansys.com/Products/Electronics/ANSYS-HFSS>), computer simulation technology (www.cst.com), etc., and their electromagnetic parameters including S-parameter or voltage standing wave ratio (VSWR) are obtained. Then, the new samples will be added into the training set to train the GP again and again until the target is reached. This is so-called PGP. Finally, the PSO algorithm is used to optimize the trained PGP and find the optimization results.
- (2) In order to verify the feasibility of the proposed PGP model, we experiment with two monopole antennas with complex structures, and the simulation results show that the proposed PGP model is effective.

The rest of the paper is organized as follows. Section “Key technical background” introduces the key technical background of GP and PSO, and then the PGP model is proposed in Section “The proposed PGP.” In Section “Simulation examples,” wideband monopole antenna and UWB MSA are optimized by the model which shows the effectiveness of the PGP. Conclusions and future studies are in Section “Conclusion.”

Key technical background

Gaussian process

A GP is defined as a set of random variables, in which any finite subset is subjected to a joint Gaussian distribution. Suppose there are N samples in training set $D, D = \{(\mathbf{x}_i, \mathbf{y}_i) | i = 1, 2, \dots, N\}$, where \mathbf{x}_i represents i -th input vector with Q dimension, and \mathbf{y}_i represents the corresponding output. All training inputs are denoted as \mathbf{X} and target outputs as \mathbf{Y} , therefore all observed data, namely training set can be denoted as $D = (\mathbf{X}, \mathbf{Y})$. From the perspective of function space, GP can be regarded as distribution of functions, where GP is completely defined by its mean function $m(\mathbf{x})$ and covariance function $k(\mathbf{x}, \mathbf{x}')$, and they are given by

$$\begin{aligned} m(\mathbf{x}) &= E[f(\mathbf{x})] \\ k(\mathbf{x}, \mathbf{x}') &= E[(f(\mathbf{x}) - m(\mathbf{x}))(f(\mathbf{x}') - m(\mathbf{x}'))]. \end{aligned} \tag{1}$$

where $f(\mathbf{x})$ is the formal expression of GP, and it is

$$f(\mathbf{x}) \sim GP(m(\mathbf{x}), k(\mathbf{x}, \mathbf{x}')) \tag{2}$$

According to the definition, joint distribution of any finite random variables in GP is Gaussian distribution, so the joint distribution of training output \mathbf{f} and test output \mathbf{f}_* is

$$\begin{bmatrix} \mathbf{f} \\ \mathbf{f}_* \end{bmatrix} \sim N\left(0, \begin{bmatrix} \mathbf{K}(\mathbf{X}, \mathbf{X}) & \mathbf{K}(\mathbf{X}, \mathbf{X}_*) \\ \mathbf{K}(\mathbf{X}_*, \mathbf{X}) & \mathbf{K}(\mathbf{X}_*, \mathbf{X}_*) \end{bmatrix}\right) \tag{3}$$

where \mathbf{K} is the covariance matrix calculated by the covariance function. The predicted distribution of test output can be obtained by Bayesian formula

$$\begin{aligned} \mathbf{f}_* | \mathbf{X}, \mathbf{f}, \mathbf{X}_* &\sim N(\mathbf{K}(\mathbf{X}_*, \mathbf{X})\mathbf{K}(\mathbf{X}, \mathbf{X})^{-1}\mathbf{f}, \\ &\mathbf{K}(\mathbf{X}_*, \mathbf{X}_*) - \mathbf{K}(\mathbf{X}_*, \mathbf{X})\mathbf{K}(\mathbf{X}, \mathbf{X})^{-1}\mathbf{K}(\mathbf{X}, \mathbf{X}_*)) \end{aligned} \tag{4}$$

In general, the training output \mathbf{Y} is not generated by a GP directly. Usually, it is in the form of noise, namely $\mathbf{Y} = f(\mathbf{x}) + \varepsilon$, where ε is additive independent identically distributed Gaussian noise with variance σ_n^2 . Given an implicit function, the likelihood of the observed data also submits to the Gaussian distribution. Then, the joint distribution of training output \mathbf{Y} and noiseless prediction output \mathbf{f}_* is

$$\begin{bmatrix} \mathbf{Y} \\ \mathbf{f}_* \end{bmatrix} \sim N\left(0, \begin{bmatrix} \mathbf{K}(\mathbf{X}, \mathbf{X}) + \sigma_n^2 \mathbf{I} & \mathbf{K}(\mathbf{X}, \mathbf{X}_*) \\ \mathbf{K}(\mathbf{X}_*, \mathbf{X}) & \mathbf{K}(\mathbf{X}_*, \mathbf{X}_*) \end{bmatrix}\right) \tag{5}$$

After re-deducing the conditional distribution, the predicted distribution of GP can be obtained as

$$\mathbf{f}_* | \mathbf{X}, \mathbf{Y}, \mathbf{X}_* \sim N(\bar{\mathbf{f}}_*, \text{cov}(\mathbf{f}_*)) \tag{6}$$

where

$$\bar{\mathbf{f}}_* = \mathbf{K}(\mathbf{X}_*, \mathbf{X})[\mathbf{K}(\mathbf{X}, \mathbf{X}) + \sigma_n^2 \mathbf{I}]^{-1} \mathbf{Y} \tag{7}$$

$$\begin{aligned} \text{cov}(\mathbf{f}_*) &= \mathbf{K}(\mathbf{X}_*, \mathbf{X}_*) \\ &- \mathbf{K}(\mathbf{X}_*, \mathbf{X})[\mathbf{K}(\mathbf{X}, \mathbf{X}) + \sigma_n^2 \mathbf{I}]^{-1} \mathbf{K}(\mathbf{X}, \mathbf{X}_*) \end{aligned} \tag{8}$$

The optimal hyper-parameters are obtained by maximizing log-likelihood function of the training sample:

$$\log p(\mathbf{f} | \mathbf{X}) = -\frac{1}{2} \mathbf{f}^T \mathbf{K}^{-1} \mathbf{f} - \frac{1}{2} \log |\mathbf{K}| - \frac{n}{2} \log 2\pi \tag{9}$$

where $\mathbf{K} = \mathbf{K}(\mathbf{X}, \mathbf{X})$, $|\mathbf{K}|$ is the determinant of \mathbf{K} , \mathbf{f} is the training target vector, \mathbf{X} is the matrix of input vector, and n is the number of hyper-parameters.

In this paper, we use squared exponential covariance function with automatic relevance determination (ARD) distance measure, and it is given by

$$k(\mathbf{x}, \mathbf{x}') = \sigma_f^2 \exp[-0.5(\mathbf{x} - \mathbf{x}')^T \mathbf{M}^{-1}(\mathbf{x} - \mathbf{x}')] \tag{10}$$

where the \mathbf{M} matrix is diagonal with ARD parameters $\lambda_1^2, \lambda_2^2, \dots, \lambda_D^2$, where D is the dimension of the input space, and σ_f^2 is the signal variance. We also use the Gaussian likelihood function for regression, and it is given by

$$\text{lik Gauss}(x) = \frac{1}{\sqrt{2\pi\sigma_n^2}} \exp\left(-\frac{(x - \mu)^2}{2\sigma_n^2}\right) \tag{11}$$

where μ is the mean and σ_n^2 is the standard deviation. Therefore, the hyper-parameters are:

$$\boldsymbol{\theta} = [\log(\lambda_1), \log(\lambda_2), \dots, \log(\lambda_D), \log(\sigma_n), \log(\sigma_f)] \tag{12}$$

Particle swarm optimization

PSO is a very popular global optimization method, and it has advantages of easy to implement, simple, fewer parameters and can effectively solve the global optimization problems [22, 23]. The velocity and position update formulas are:

$$v_{i,d}^{k+1} = \omega v_{i,d}^k + c_1 \text{rand}() (p_{i,d}^k - x_{i,d}^k) + c_2 \text{rand}() (p_{g,d}^k - x_{i,d}^k) \tag{13}$$

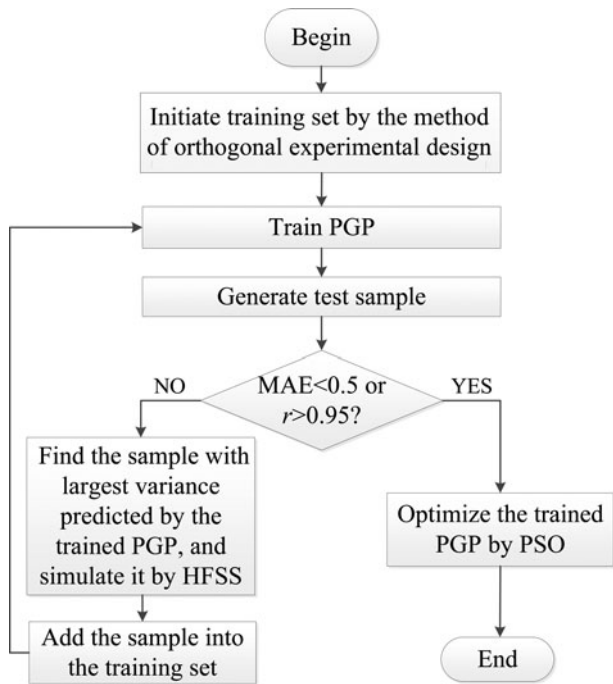


Fig. 1. Flow chart of the proposed PGP.

$$x_{i,d}^{k+1} = x_{i,d}^k + v_{i,d}^{k+1} \tag{14}$$

where c_1 and c_2 are learning factors and usually $c_1 = 2$ and $c_2 = 2$. $\text{rand}()$ is a random number between 0 and 1. ω is the inertia weight, usually it is linearly decreasing, namely

$$\omega = 0.9 - (0.9 - 0.4) \times (\text{generation}/\text{maxgeneration})^2$$

where maxgeneration is the maximum iteration number, and generation is the current iteration number. $v_{i,d}^k$ and $x_{i,d}^k$ are velocity and position of d -dimensional i -th particle in the k -th iteration. $p_{i,d}^k$ is the personal best position and $p_{g,d}^k$ is the global best position.

The proposed PGP

The flow chart of the proposed PGP model based on PSO algorithm is shown in Fig. 1, and the main steps are as follows:

- (1) To a designed antenna, select samples using the method of orthogonal experimental design [24], and then call full-wave electromagnetic simulation software HFSS to compute the S-parameter or VSWR. After that, we obtain the training set.
- (2) Use the size parameters of the designed antenna and frequency points as inputs, and S-parameter or VSWR as output to train the GP model.
- (3) Randomly generate a test sample, and then compute mean absolute error (MAE) and correlation coefficient (r) between GP predicted result and HFSS simulation one. If $\text{MAE} < 0.5$ and $r > 0.95$ in this paper, go to step 5, otherwise go to step 4.
- (4) Randomly generate some test samples and evaluate them by the trained GP model, and obtain their predicted mean m and variance σ^2 . Then select the sample with large variance, and simulate S-parameter or VSWR by calling HFSS. Finally, the sample is added to the training set. Progressively, we train the GP again, after that go to step 3.

- (5) The trained PGP model is used as the fitness function of PSO algorithm to optimize the antenna:

$$\text{MAE} = \frac{1}{j} \sum_{i=1}^j |y_i - \hat{y}_i| \tag{15}$$

$$r = \frac{\sum_{i=1}^j (\hat{y}_i - \bar{\hat{y}})(y_i - \bar{y})}{\sqrt{\sum_{i=1}^j (\hat{y}_i - \bar{\hat{y}})^2 \sum_{i=1}^j (y_i - \bar{y})^2}} \tag{16}$$

where j represents the size of vector y , y_i represents the HFSS simulation value, \hat{y}_i represents the PGP predicted value, $\bar{\hat{y}}$ represents mean of the PGP predicted value, and \bar{y} represents mean of the HFSS simulation value. In this paper, the difference between the PGP-predicted result and HFSS simulation result is showed by the correlation coefficient r and MAE. If r is closer to 1 or MAE is closer to 0, then the model is more reasonable.

In addition, for the proposed PGP, training time complexity is $O(n^3)$ and spatial complexity is $O(n^2)$, where n is the number of selected frequency points. This paper also uses sparse sampling method which we sample intensively in important frequency range and sparsely in the secondary frequency range. Therefore, we only need m ($m < n$) points to fit prediction performance.

Simulation examples

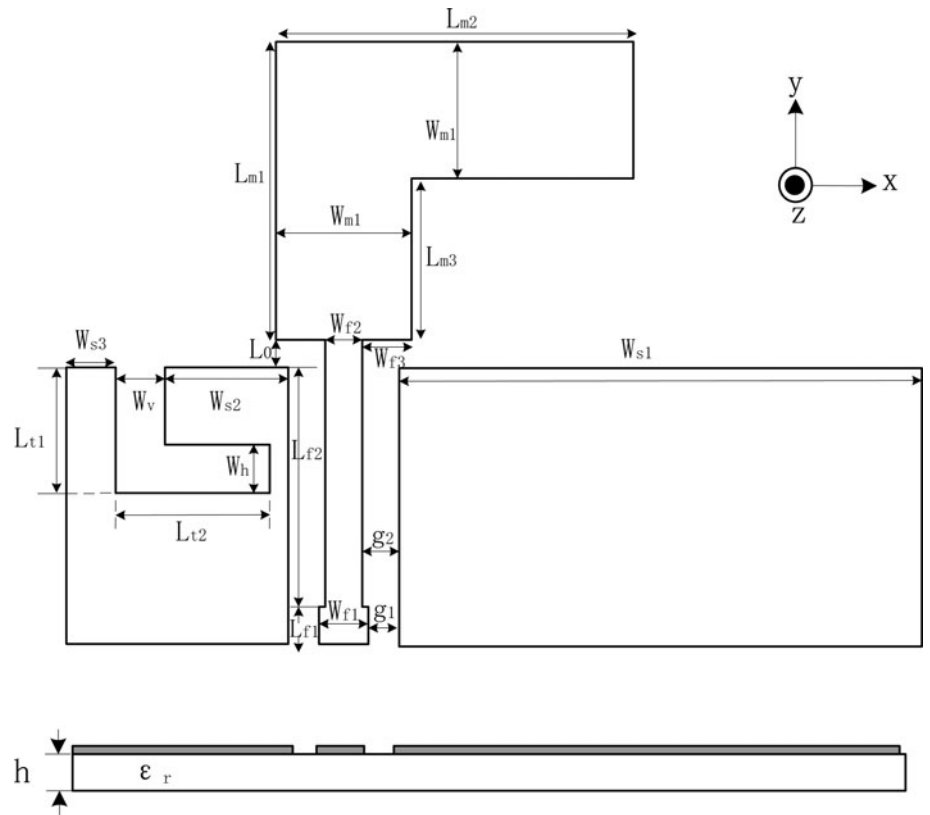
Wideband monopole antenna

The proposed PGP is applied to optimize the wideband monopole antenna based on CPW-fed step impedance in [25] as the first example, shown in Fig. 2. The MSA is fabricated on an FR4 microwave substrate with $56.47 \times 53.44 \text{ mm}^2$, thickness of 0.8 mm, relative dielectric constant of 4.4, and loss tangent of 0.02. We will optimize the antenna performance by changing the geometry of the L-shaped slot and the ground plane to satisfies the following design specifications:

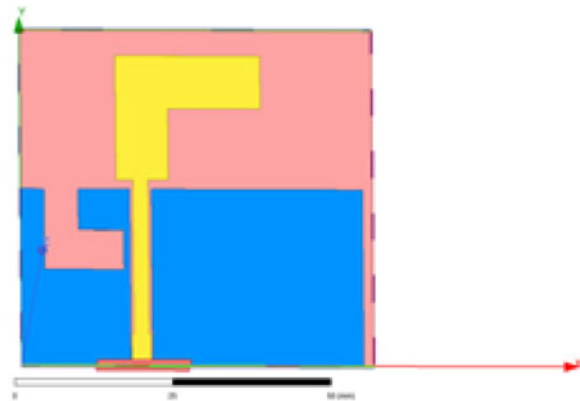
$$\begin{aligned} |S_{11}| &\leq -10 \text{ dB for } 1.5 \text{ through } 2.8 \text{ GHz} \\ |S_{11}| &\leq -10 \text{ dB for } 4.6 \text{ through } 6.1 \text{ GHz} \end{aligned}$$

The fixed sizes of the antenna are $L_{m1} = 19.7 \text{ mm}$, $L_{m2} = 23.2 \text{ mm}$, $L_{m3} = 11.3 \text{ mm}$, $L_{l2} = 12.75 \text{ mm}$, $L_{f1} = 5 \text{ mm}$, $L_{f2} = 23 \text{ mm}$, $L_0 = 1.5 \text{ mm}$, $W_{f1} = 3 \text{ mm}$, $W_{f2} = 2.4 \text{ mm}$, $W_{f3} = 3 \text{ mm}$, $W_{s2} = 8.25 \text{ mm}$, $W_{s3} = 3.75 \text{ mm}$, $W_{m1} = 8.4 \text{ mm}$, $W_v = 5.5 \text{ mm}$, $g_1 = 0.25 \text{ mm}$, $g_2 = 0.55$, $h = 0.8 \text{ mm}$. The widths of the two quasi-transmission lines are 2.4 mm (W_{f2}) and 8.4 mm (W_{m1}). In order to demonstrate the impedance characteristics of the proposed monopole antenna, the design parameters $x = [L_{t1}, W_{s1}, W_h] \text{ mm}$ are selected for optimization because they are the main factors that impact the performance of the antenna. Table 1 shows the ranges of x .

First, we select nine groups x as initial samples by partial orthogonal table ($L_9(3^4)$) and simulate their S-parameters by using HFSS software in the frequency range 1.4–6.6 GHz with an interval of 0.05 GHz. In this example, sparse sampling method, with frequency interval of 0.1 GHz from 1.4 to 2.9 GHz, 0.3 GHz from 3 to 4.5 GHz, and 0.2 GHz from 4.6 to 6.6 GHz, is adopted for training. Therefore, we select $m = 33$ rather than $n = 105$ frequency points. The PGP is trained by the nine group samples with x and 33 frequency points as input and their corresponding S-parameters as output. Table 2



(a) Schematic diagram



(b) HFSS model

Fig. 2. Wideband monopole antenna (a) schematic diagram and (b) HFSS model.

Table 1. Parameter ranges of the wideband monopole antenna

Parameter	L_{t1}	W_{s1}	W_h
Unit (mm)	[12.4,14.4]	[28,34]	[5,7]

Table 2. Results of different updating numbers for the wideband monopole antenna

Number	MAE	r
0	0.7670	0.9368
1	0.5379	0.9938
2	0.9598	0.9699
3	0.6972	0.9805
4	0.4305	0.9932

shows the MAE and r during modeling process. The r and MAE between the initial GP model (the number is 0 in Table 2) and HFSS are 0.9368 and 0.7670, respectively. After updating four times, the correlation coefficient r increases from 0.9368 to 0.9932, while the MAE decreases from 0.7670 to 0.4305, which satisfies the threshold. The hyper-parameters of the trained PGP are

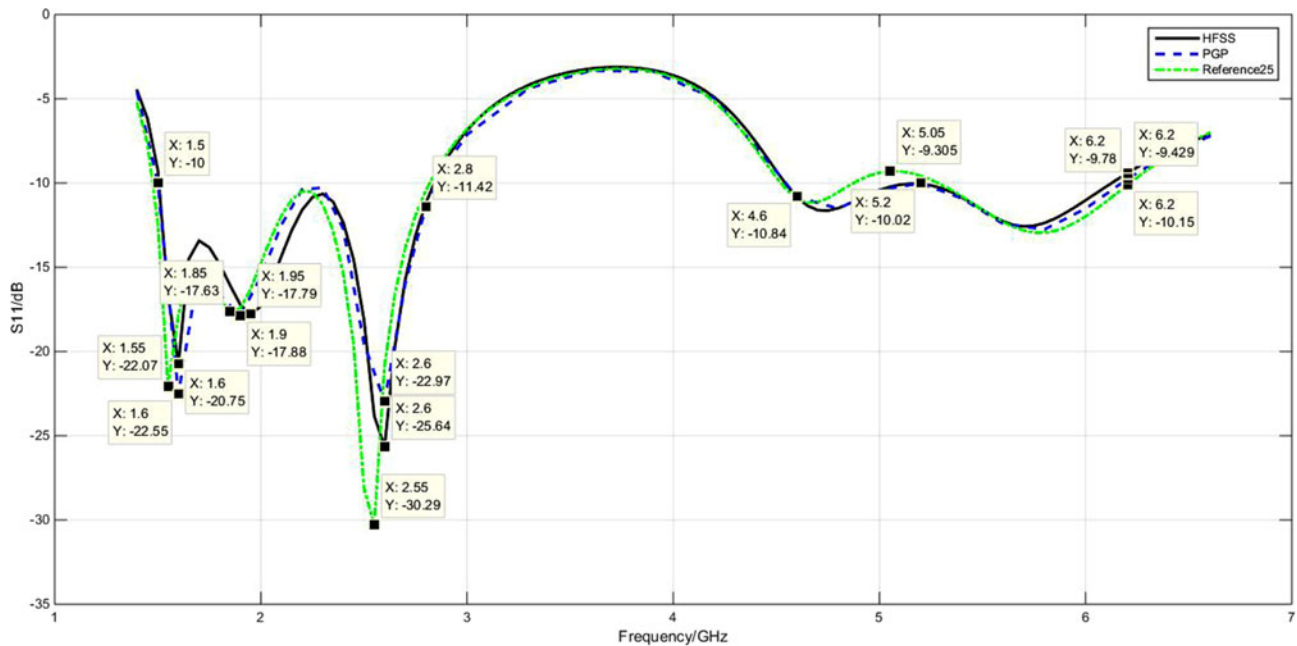


Fig. 3. Comparison result of the trained PGP, HFSS, and [25] for the wideband monopole antenna.

$$\theta = [\log(\lambda_1), \log(\lambda_2), \log(\lambda_3), \log(\lambda_4), \log(\sigma_f)]$$

$$= [10.85, 2.9425, 11.0159, -2.4772, 2.3175].$$

We use the trained PGP exploiting PSO to optimize the wideband monopole MSA, with the maximum iteration number of the PSO is 300, $c1 = c2 = 2$ and swarm size is 20. In this example, to satisfy the antenna design specifications, the fitness function of the PSO is given by

$$Fit = \sum_i^{len(freq)} \frac{1}{len(freq)} |y_{pgp,i} - y_{hfss,i}|$$

s.t. $|y_{@1.5\text{ GHz}}| > 10 \&\& |\max(y_{@1.6\text{ GHz}}, y_{@2.0\text{ GHz}}, y_{@2.6\text{ GHz}})| > 10$
 $\&\& |y_{@2.8\text{ GHz}}| > 10 \&\& |y_{@4.6\text{ GHz}}| > 10 \&\& |y_{@6.1\text{ GHz}}| > 10$
 $\&\& |\max(y_{@5.2\text{ GHz}}, y_{@5.8\text{ GHz}})| > 10$

(17)

where $len(freq)$ is the number of points over frequency band, $y_{pgp,i}$ is the predicted value by the trained PGP model at the i -th frequency point, $y_{hfss,i}$ is the simulated value of HFSS software at the i -th frequency point, $y_{@1.5\text{ GHz}}$ is the $|S_{11}|$ at the 1.5 GHz, and the notation $\&\&$ means that all conditions must be met simultaneously.

After optimization, the result is $x = [13.0505, 30.4825, 5.3912]$ mm.

The comparison result of the proposed PGP and HFSS is shown in Fig. 3, where the solid line represents simulation result based on HFSS software, the dashed line represents predicted result given by the trained PGP model, and the dotted line represents the result in [25].

We can conclude from Fig. 3 that the optimized result by the trained PGP exploiting PSO basically satisfies the design requirements. Meanwhile, at the three resonant frequency points, the deviation value is also within the acceptable range. The reason why the proposed PGP model is more effective compared to

the GP model is that training samples for the PGP are more targeted and progressive. It benefits from the samples, reducing the computing time of covariance matrix for unnecessary training samples.

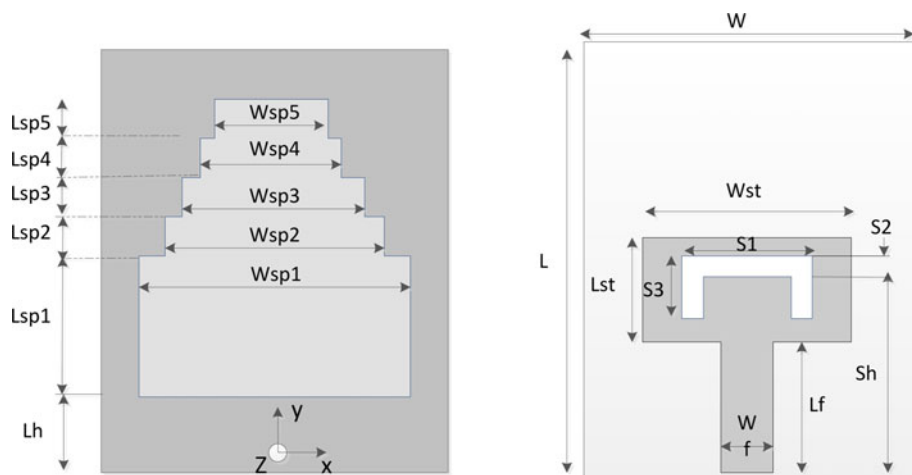
From the perspective of calculation time, if the antenna is optimized by PSO evaluated by HFSS, it takes about 5 min for one evaluation, while it will take about 30 000 min for 20 particles to iterate 300 times. However, for the proposed PGP model, the total time, including the time to obtain training samples by HFSS, progressively training time, and optimal time based on the trained PGP model, is about 85 min. The efficiency is very high.

UWB monopole antenna

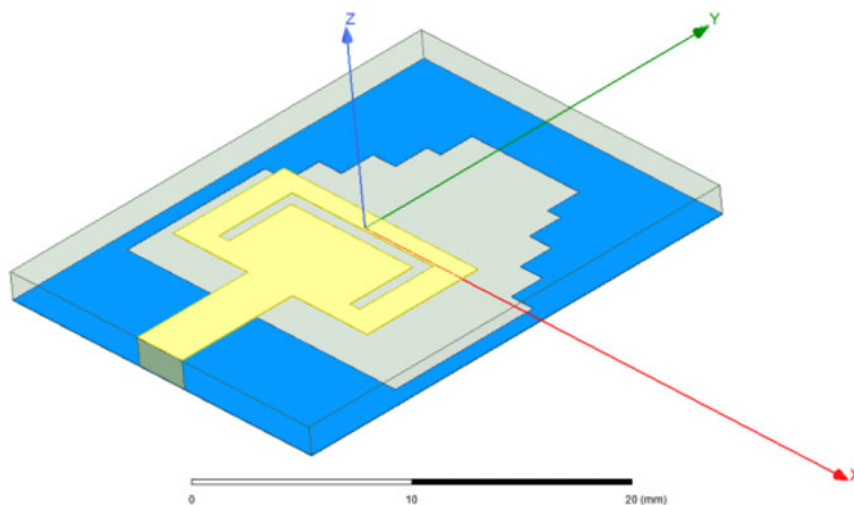
In this subsection, we optimize a compact step-slot monopole antenna with band-notched characteristics for UWB applications [26] based on the proposed PGP model and PSO. The MSA can obtain frequency notch characteristic in the WLAN band, and band-notched characteristic is achieved by introducing an inverted-U slot into the rectangular stub. The schematic diagram of the MSA is shown in Fig. 4, which has a compact size of $20 \times 26\text{ mm}^2$ ($W \times L$), fabricated on the FR4 dielectric substrate with the thickness of 1.6 mm, relative dielectric constant of 4.4, fed by a microstrip line with the rectangular stub and a step-slot which are printed on the different side of the dielectric substrate. The design specifications are as follow:

- VSWR < 2 for 3.1–5 GHz
- VSWR > 2 for 5–6 GHz
- VSWR < 2 for 6–10.6 GHz

The fixed size are $W_{sp1} = 18\text{ mm}$, $W_{sp2} = 15\text{ mm}$, $W_{sp3} = 12\text{ mm}$, $W_{sp4} = 9\text{ mm}$, $W_{sp5} = 7.2\text{ mm}$, $W = 20\text{ mm}$, $L = 26\text{ mm}$, $L_{sp1} =$



(a) Schematic diagram



(b) HFSS model

Fig. 4. UWB MSA: (a) schematic diagram and (b) HFSS model.

Table 3. Parameter ranges of the UWB MSA

Parameter	S_1	S_2	S_3	S_h
Unit (mm)	[9,11.5]	[0.5,0.9]	[3,4.2]	[11.75,12.75]

8.75 mm, $L_{sp2} = 2$ mm, $L_{sp3} = 2$ mm, $L_{sp4} = 2$ mm, $L_{sp5} = 2$ mm, $W_{st} = 13$ mm, $L_{st} = 7$ mm, $W_f = 3$ mm, $L_f = 7$ mm, and $L_h = 6.25$ mm. The selected variables is $\mathbf{x} = [S_1, S_2, S_3, S_h]$ that determines the position and size of the inverted-U slot, and their ranges are shown in Table 3.

We also select nine groups x as initial samples by partial orthogonal table ($L_9(3^4)$), and then simulate their VSWR by using HFSS software. The frequency range is 3–12 GHz with an interval of 0.1 GHz. In this example, sparse sampling method, with frequency interval of 0.2 GHz from 3.1 to 4.5 GHz, 0.1 GHz from 4.6 to 6.7 GHz, and 0.4 GHz from 6.8 to 12 GHz, is also adopted. Therefore, we select $m = 43$ rather than $n = 91$ frequency points. The proposed PGP is trained, and MAE and r are shown in Table 4 simultaneously. The correlation coefficient r between original GP (the number is 0 in Table 4) and HFSS

Table 4. Results of different updating numbers for the UWB MSA

Number	MAE	r
0	0.8457	0.5130
5	0.6388	0.7859
10	0.5457	0.7409
15	0.4254	0.9228
21	0.2893	0.9575

is 0.5130, and MAE is 0.8457. After updating 21 times, r increases from 0.5130 to 0.9575, and MAE decreases from 0.8457 to 0.2893. At this time, the hyper-parameters of the trained PGP are

$$\theta = [\log(\lambda_1), \log(\lambda_2), \log(\lambda_3), \log(\lambda_4), \log(\lambda_5), \log(\sigma_f)] \\ = [-1.5871, -1.2109, -1.3032, 0.0398, -1.9395, 0.602].$$

We use the trained PGP exploiting PSO to optimize the UWB monopole antenna, and the parameter settings are the same as the

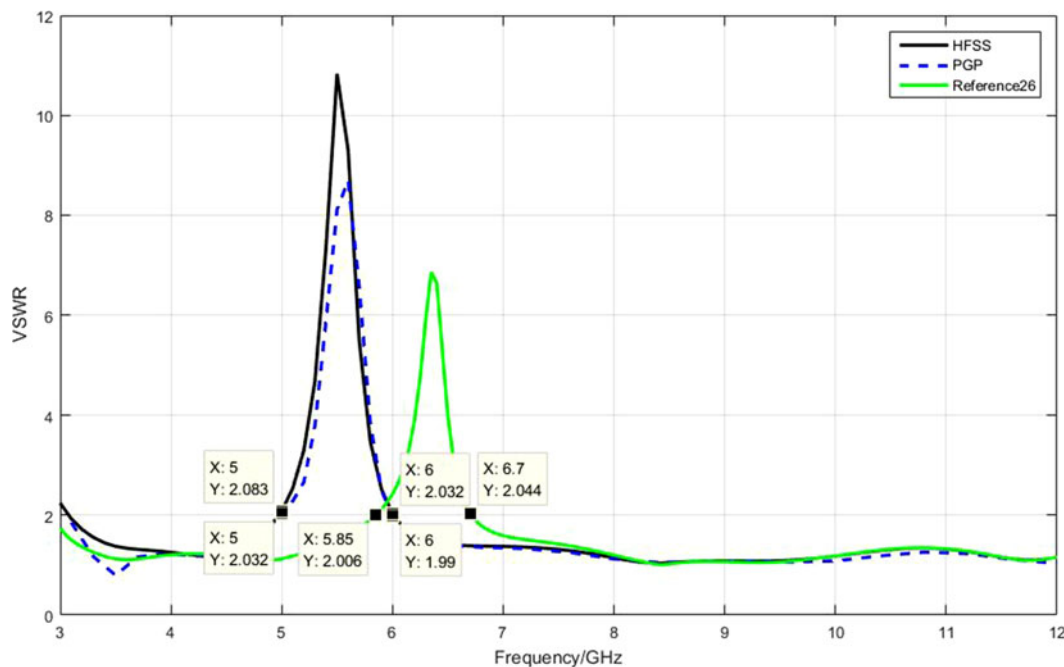


Fig. 5. Comparison result of the trained PGP, HFSS, and [26] for the UWB MSA.

last example. The fitness function is given by

$$Fit = \sum_{i=1}^{len(freq)} \frac{1}{len(freq)} |y_{pgp,i} - y_{hfss,i}|$$

$$\text{s.t. } y_{@3.1 \text{ GHz}} < 2 \ \&\& y_{@4.9 \text{ GHz}} < 2 \ \&\& y_{@5.1 \text{ GHz}} > 2$$

$$\&\& y_{@5.9 \text{ GHz}} > 2 \ \&\& y_{@6.1 \text{ GHz}} < 2 \ \&\& y_{@10.6 \text{ GHz}} < 2$$
(18)

And the optimized result is $\mathbf{x} = [10.4721, 0.8204, 3.1883, 12.1718]$ mm.

The comparison of the proposed PGP, HFSS, and [26] is shown in Fig. 5, where the solid line represents HFSS simulation result, the dashed line represents optimization result based on the trained PGP model, and the dotted line represents the result from reference [26]. Figure 5 shows the simulated impedance bandwidth for VSWR is < 2 covering from 3.1 GHz to > 12 GHz, which frequency band from 5.05 to 6.05 GHz is rejected. From the perspective of calculation time, if we optimize the antenna by using the PSO algorithm exploiting HFSS, the calculation time for one evaluation is 85 s, then the total consumed time is about 510 000 s with 20 particles and 300 iterations. However, the total time for the PGP modeling and PSO optimizing is 3360 s, which means the method is very efficient.

Conclusion

A novel surrogate model for antenna optimization design based on PGP is proposed. The method exploits the predicted variance characteristics of trained GP to obtain more valuable training samples during the modeling process. As we all know, for a general GP, we usually determine the training set at one time, for which we do not know the suitable number of the training data; moreover, we also do not know whether the data in the training set are the most effective ones for training the GP or not. The proposed PGP can answer two questions simultaneously. Taking wideband

and UWB monopole antennas as an example, the predicted result by the trained PGP model is comparable to that of the HFSS solver. The quality of the model is sufficient to be surrogate one for antenna optimization. Compared with the traditional optimization algorithms, the efficiency of the proposed method is very high.

Acknowledgements. This study is supported by the National Natural Science Foundation of China (NSFC) under No. 61771225, and the scientific research capacity improvement project of key developing disciplines in Guangdong Province of China under No. 2021ZDJ057.

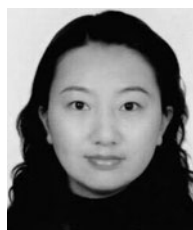
References

- Jin N and Rahmat-Samii Y (2007) Advances in particle swarm optimization for antenna designs: real-number, binary, single-objective and multi-objective implementations. *IEEE Transactions on Antennas and Propagation* 55, 556–567.
- Tian YB and Qian J (2005) Improve the performance of a linear array by changing the spaces among array elements in terms of genetic algorithm. *IEEE Transactions on Antennas and Propagation* 53, 2226–2230.
- Deb A, Roy JS and Gupta B (2014) Performance comparison of differential evolution, particle swarm optimization and genetic algorithm in the design of circularly polarized microstrip antennas. *IEEE Transactions on Antennas and Propagation* 62, 3920–3928.
- Koziel S, Ogurtsov S, Zieniutycz W and Bekasiewicz A (2014) Design of a planar UWB dipole antenna with an integrated balun using surrogate-based optimization. *IEEE Antennas and Wireless Propagation Letters* 14, 366–369.
- Liu B, Yang H and Lancaster MJ (2017) Global optimization of microwave filters based on a surrogate model-assisted evolutionary algorithm. *IEEE Transactions on Microwave Theory and Techniques* 65, 1976–1985.
- Jin J, Zhang C, Feng F, Na W, Ma J and Zhang QJ (2019) Deep neural network technique for high-dimensional microwave modeling and applications to parameter extraction of microwave filters. *IEEE Transactions on Microwave Theory and Techniques* 67, 4140–4155.
- Tian YB, Zhang SL and Li JY (2011) Modeling resonant frequency of microstrip antenna based on neural network ensemble. *International Journal of Numerical Modelling: Electronic Networks, Devices and Fields* 24, 78–88.

8. **Prado DR, Lopez JA, Barquero G, Arrebola M and Las HF** (2018) Fast and accurate modeling of dual-polarized reflectarray unit cells using support vector machines. *IEEE Transactions on Antennas and Propagation* **66**, 1258–1270.
9. **Sun FY, Tian YB, Hu GB and Shen Q Y** (2019) DOA estimation based on support vector machine ensemble. *International Journal of Numerical Modelling: Electronic Networks, Devices and Fields* **32**, e2614.
10. **Rasmussen CE and Williams CKI** (2006) Gaussian processes for machine learning. *International Journal of Neural Systems* **11**, 14.
11. **Wu Q, Wang H and Hong W** (2020) Multistage collaborative machine learning and its application to antenna modeling and optimization. *IEEE Transactions on Antennas and Propagation* **68**, 3397–3409.
12. **Chen F and Tian YB** (2014) Modeling resonant frequency of rectangular microstrip antenna using CUDA-based artificial neural network trained by particle swarm optimization algorithm. *Applied Computational Electromagnetics Society Journal* **29**.12.
13. **Chen Y, Tian YB and Le M** (2017) Modeling and optimization of microwave filter by ADS-based KBNN. *International Journal of RF and Microwave Computer-Aided Engineering* **27**, e21062.
14. **Angiulli G, Cacciola M and Versaci M** (2007) Microwave devices and antennas modelling by support vector regression machines. *IEEE Transactions on Magnetics* **43**, 1589–1592.
15. **Sun FY, Tian YB and Ren ZL** (2016) Modeling the resonant frequency of compact microstrip antenna by the PSO-based SVM with the hybrid kernel function. *International Journal of Numerical Modelling: Electronic Networks, Devices and Fields* **29**, 1129–1139.
16. **Jacobs JP and De Villiers JP** (2010) Gaussian-process-regression based design of ultrawideband and dual-band CPW-fed slot antennas. *Journal of Electromagnetic Waves and Applications* **24**, 1763–1772.
17. **Gao J, Tian YB and Chen XZ** (2020) Antenna optimization based on co-training algorithm of Gaussian process and support vector machine. *IEEE Access* **8**, 211380–211390.
18. **Zhang XY, Tian YB and Zheng X** (2020) Antenna optimization design based on deep Gaussian process model. *International Journal of Antennas and Propagation* **4**, 1–10.
19. **Chen XZ, Tian YB, Zhang TL and Gao J** (2020) Differential evolution based manifold Gaussian process machine learning for microwave filter's parameter extraction. *IEEE Access* **8**, 146450–146462.
20. **Gao J, Tian YB, Zheng X and Chen XZ** (2020) Resonant frequency modeling of microwave antennas using Gaussian process based on semi-supervised learning. *Complexity* **2020**, 6450–6462.
21. **Zhou Z, Ong YS, Nair PB, Keane AJ and Lum KY** (2006) Combining global and local surrogate models to accelerate evolutionary optimization. *IEEE Transactions on Systems, Man, and Cybernetics, Part C* **37**, 66–76.
22. **Kennedy J and Eberhart R** (1995) Particle swarm optimization. *IEEE International Conference on Neural Networks, Perth, WA, Australia*, pp. 1942–1948.
23. **Tian YB** (2014) *Particle Swarm Optimization and Application in Electromagnetics*. Beijing, China: Science Press.
24. **William G and Gertrude MC** (1992) *Experimental Designs*, 2nd Edn. Wiley, USA: Soil Science Society of America Journal.
25. **Wang CJ and Hsu CW** (2017) A microstrip wideband monopole antenna for multisystem integration by utilizing stepped-impedance structure and L-shaped slot. *International Journal of RF and Microwave Computer-Aided Engineering* **27**, e21086.
26. **Thaiwirot W, Chareonsiri Y and Akkaraekthalin P** (2015) A compact band-notched step-slot antenna for UWB applications. *IEEE Conference on Antenna Measurements and Applications (CAMA), Chiang Mai, Thailand*, pp. 1–4.



Xie Zheng was born in Liyang, Jiangsu province, China, in 1994. He is a graduate student at the Jiangsu University of Science and Technology. His research interest is in rapid optimization design of electromagnetic microwave devices.



Fei Meng was born in Shenyang, Liaoning province, China, in 1977. She is currently with the School of Information and Communication Engineering, Guangzhou Maritime University, Guangzhou, China. She has authored and coauthored 10 journal papers. Her research interest is in surrogates and their applications.



Yubo Tian was born in Tieling, Liaoning province, China, in 1971. He received his Ph.D. degree in radio physics from the Department of Electronic Science and Engineering, Nanjing University, Nanjing, China. He had been a visiting scholar at the University of California Los Angeles in 2009 and the Griffith University in 2015, respectively. From 1997 to 2004, he was with the Department of Information Engineering, Shenyang University, Shenyang, China. From 2005 to 2020, he was with the School of Electronics and Information, Jiangsu University of Science and Technology, Zhenjiang, China, where he was a full professor and vice Dean from 2011. He is currently with the School of Information and Communication Engineering, Guangzhou Maritime University, Guangzhou, China. Dr. Tian has authored and coauthored more than 100 journal papers and three books. He also holds more than 20 filed/granted patents in China. His current research interest is in machine-learning methods and their applications in electronics and electromagnetics.



Xinyu Zhang was born in Yangzhou, Jiangsu province, China, in 1994. He is a graduate student at the Jiangsu University of Science and Technology. His research interest is in deep learning methods and their application in electromagnetic microwave devices.